

Measurements of Gain Larger than 10^5 at $12 \mu\text{m}$ in a Self-Amplified Spontaneous-Emission Free-Electron Laser

M. J. Hogan, C. Pellegrini, J. Rosenzweig, S. Anderson, P. Frigola, and A. Tremaine
Department of Physics and Astronomy, UCLA, Los Angeles, California 90095

C. Fortgang, D. C. Nguyen, R. L. Sheffield, and J. Kinross-Wright
Los Alamos National Laboratory, Los Alamos, New Mexico 87545

A. Varfolomeev, A. A. Varfolomeev, and S. Tolmachev
RRC–Kurchatov Institute, Moscow, Russia

Roger Carr

Stanford Synchrotron Radiation Laboratory, Palo Alto, California 94304

(Received 29 April 1998)

We report measurements of very large output intensities corresponding to a gain larger than 10^5 for a single pass free-electron laser operating in the self-amplified spontaneous emission (SASE) mode at $12 \mu\text{m}$. We also report the observation and analysis of intensity fluctuations of the SASE radiation intensity in the high-gain regime. The results are compared with theoretical predictions and simulations. [S0031-9007(98)07403-1]

PACS numbers: 41.60.Cr, 41.60.Ap

Powerful sources of coherent x rays, based on free-electron lasers (FELs) operating in the self-amplified spontaneous emission (SASE) mode and driven by high energy, high brightness electron beams, are being designed in the United States and Europe [1,2]. These projects require experimental verification to validate the theoretical predictions for a SASE-FEL. Experimental results showing SASE with a gain of many orders of magnitude were first obtained at a wavelength of 8 mm propagating in a waveguide [3]. More recently, experimental results have been obtained by several groups in the infrared [4,5] and visible [6] with gains of about 1 order of magnitude or less and another with a gain of about 300 [7]. In this paper we report experimental data showing a gain of 3×10^5 at $12 \mu\text{m}$. This is the largest gain to date at an optical wavelength for a SASE-FEL. We have also measured and analyzed the fluctuations of the output intensity from pulse to pulse. The data on intensity and intensity fluctuations are compared with the theory of a SASE-FEL and are found to be in good agreement [8–10].

When an electron beam passes through a planar undulator of period λ_u and undulator parameter K , it produces radiation at the wavelength $\lambda = (\lambda_u/2\gamma^2)[1 + (K^2/2)]$, where γ is the electron energy in rest mass units and K is the undulator vector potential normalized to mc^2 . If the electron beam has a large phase space density an instability develops, and the output power grows exponentially along the undulator axis z . For an undulator long compared to the FEL gain length L_g , the radiation intensity is given by $i = (i_0/9)C \exp(2z/L_g)$, where i_0 is the spontaneous undulator radiation intensity emitted in the first gain length and C is a factor describing the coupling between

the spontaneous radiation and the amplified mode. In the simple one dimensional (1D) theory, neglecting diffraction and slippage, the field gain length is given by $L_g = \lambda_u/2\sqrt{3} \pi \rho$, where the FEL parameter ρ is proportional to the beam plasma frequency to the power of $\frac{2}{3}$, or $(Q/\sigma^2 L_b)^{1/3}$. Here Q is the charge in an individual electron bunch, σ the beam radius, and L_b the bunch length. Saturation occurs after about 10 field gain lengths and the radiation intensity at saturation is about ρ multiplied by the beam energy. Diffraction, energy spread (σ_E), and slippage $S = N_u \lambda$ can all increase the gain length over the 1D value if the conditions $\varepsilon \leq \lambda/4\pi$, $\sigma_E/E < \rho$, $S < L_b$, and $Z_R > L_g$ are not satisfied, where ε is the beam emittance, N_u the number of undulator periods, and Z_R the Rayleigh range [8–10].

The spontaneous radiation intensity is proportional to $|j(\omega)|^2$, where $j(\omega)$ is the Fourier component of the longitudinal beam density distribution at the frequency $\omega = 2\pi c/\lambda$. For our case, when the beam is produced by a photocathode and the bunch length is much larger than λ , $j(\omega)$ is a random number with $\langle j(\omega) \rangle = 0$ and $\langle |j(\omega)|^2 \rangle \sim Q$. Hence the output intensity is also a random number proportional to the charge and fluctuates from pulse to pulse. These fluctuations have been observed for a short undulator with no FEL gain [11] and for SASE [4,6] in the infrared and visible. Here we extend these measurements of the intensity distribution of a SASE-FEL to a region of large gain.

This experiment was conducted using the Advanced Free Electron Laser (AFEL) linac [7] at the Los Alamos National Laboratory in conjunction with a 2 m long University of California Los Angeles–Kurchatov Institute of

Atomic Energy undulator. The AFEL linac is a 10.5 cell L -band structure with a CsTe₂ photocathode at one end. The photocathode is driven by an 8 ps frequency quadrupled Nd:YLF laser, producing a series of electron micropulses about 10 ps long separated by 9.23 ns. The linac rf power system produces macropulses up to 10 μ s long repeating at 1 Hz. For every rf macropulse in the linac, there are several hundred individual electron micropulses. By changing the drive laser intensity, the charge in an individual micropulse can be changed from a few hundred pC to several nC.

This bright electron beam is matched into the undulator with a focusing solenoid located around the photocathode and another 30 cm before the undulator. The average charge in a macropulse is measured at beam position monitors (BPMs) before and after the undulator. The electron beam radius and pulse length are measured using optical transition radiation (OTR). OTR generated before the entrance of the undulator is sent to a streak camera to determine the electron beam pulse length that, divided into the charge, gives the peak current. The OTR from three different longitudinal positions within the undulator was used to measure the transverse beam size and thus the current density. Note that both the average electron beam radius ($\sqrt{\sigma_x \sigma_y}$) and pulse length (L_b) vary as a function of charge as shown in Fig. 1. The fits for both spot size and pulse length follow the same functional form [12] $y = \sqrt{a^2 + (bQ)^2}$, where Q is the charge in nC. For the spot size, the constants are $a = 120 \mu\text{m}$, $b = 38 \mu\text{m/nC}$, and for pulse length $a = 3 \text{ ps}$, $b = 2.2 \text{ ps/nC}$. The energy and energy spread are measured with a dipole spectrometer after the exit of the undulator. The uncorrelated energy spread is 0.25% for the beam core at a charge of 2 nC and larger if we include the tail of the distribution. The energy spread for beam charges smaller than 2 nC has not been measured; however, it can only decrease with charge. Simulations using PARMELA show an energy spread decreasing lin-

early with charge under our conditions. The measured values of electron beam parameters are given in Table I.

The 2 m long permanent magnet undulator, constructed at UCLA, has equal focusing in both planes, and a betatron wavelength of 1.2 m. The horizontal focusing is obtained with quadrupole magnets located around the main undulator magnets, providing a longitudinally uniform horizontally focusing field equal to the sum of the natural focusing and the vertically defocusing quadrupole field in the vertical plane. The magnetic field quality was measured using the pulsed wire technique and corrected with shimming magnets. After correction the final rms field error is less than 0.5%, and the electron trajectory deviates from the ideal trajectory by less than one wiggles amplitude (100 μm). The undulator parameters are listed in Table I and a plot of the electron beam trajectory as measured with the wire system is shown in Fig. 2.

Two sets of measurements of the FEL output intensity have been done: one averaging over all of the micropulses to determine the average radiation intensity as a function of charge, the other measuring the radiation from individual micropulses with the same charge to determine the intensity fluctuations. In the first case, a single rf macropulse, consisting of several hundred individual micropulses, was generated and sent through the undulator. The charge was measured nondestructively with the BPMs and the radiated intensity was measured with a slow ($\sim 100 \text{ ns}$ response time) liquid nitrogen cooled HgCdTe detector. The drive laser intensity on the photocathode was changed (thus changing the charge) and the measurements were repeated, adding optical attenuators as necessary to avoid saturating the IR detector. At 2.2 nC, the SASE output was detectable with a calibrated energy meter that, when compared with the HgCdTe signal and combined with the value of the attenuators, provided an absolute energy measurement at all charge levels. The FEL intensity is measured in a solid angle equal to Ω_c , where $\Omega_c = \pi \lambda / L_u$ is the coherent solid angle and L_u the undulator length. The average FEL output

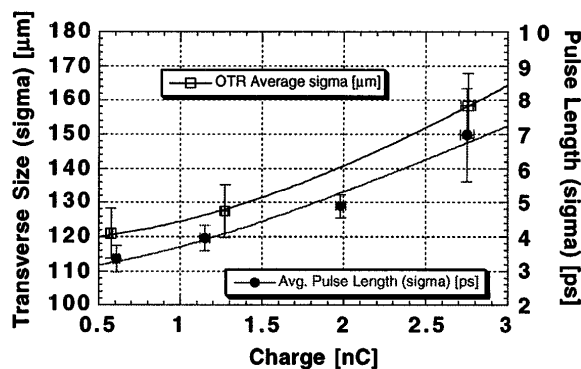


FIG. 1. Measured electron beam transverse size (μm) and pulse length (ps) as a function of micropulse charge (nC). The fits for both spot size and pulse length follow the same functional form $y = \sqrt{a^2 + (bQ)^2}$, where Q is the charge in nC. For the spot size, the constants are $a = 120 \mu\text{m}$, $b = 38 \mu\text{m/nC}$, and for pulse length $a = 3 \text{ ps}$, $b = 2.2 \text{ ps/nC}$.

TABLE I. Electron beam, undulator, and FEL characteristics.

Electron Beam	
Energy [MeV]	18
Charge per micropulse [nC]	0.3–2.2
Transverse spot size (σ) [μm]	115–145
Uncorrelated energy spread at 2 nC (σ) [%]	0.25
Pulse length (σ) [ps]	3–5.5
Peak current [A]	40–170
Undulator	
Period [cm]	2.05
Number of periods	98
Undulator parameter (K)	1.04
Betatron wavelength [m]	1.2
FEL	
Radiation wavelength [μm]	12
Field gain length at 2.2 nC [cm]	25

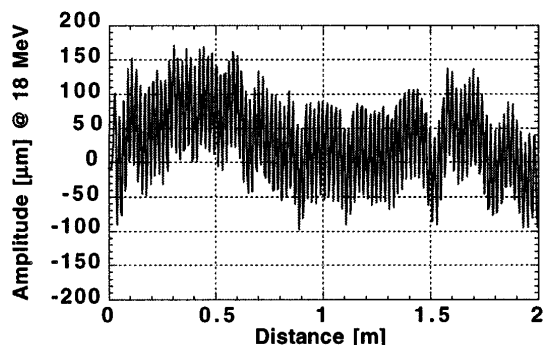


FIG. 2. Electron beam wobble-plane trajectory through the undulator as predicted by the pulsed wire measurements.

intensity is plotted versus average micropulse charge in Fig. 3. The measured gain was critically dependent on the electron beam alignment, focusing, and drive laser-rf phase and shows no evidence of the Q^2 dependence indicative of coherent spontaneous emission.

For the beam parameters given in Table I, the Rayleigh range is less than the gain length and the slippage is comparable to the bunch length, so we must include slippage [13] and diffraction effects (gain guiding), as well as the charge dependence of the beam radius and bunch length. Because no simple analytic model takes all of these effects into account, we use the code GINGER [14] to evaluate the theoretical FEL intensity. The GINGER simulations are done with spot sizes and pulse lengths obtained from the fits to the data shown in Fig. 1. As we have measured only the energy spread for a charge of 2 nC, we use this value of 0.25% for all the simulations shown in Fig. 4. Using the data for spot size and pulse length, we have evaluated the FEL parameter ρ and

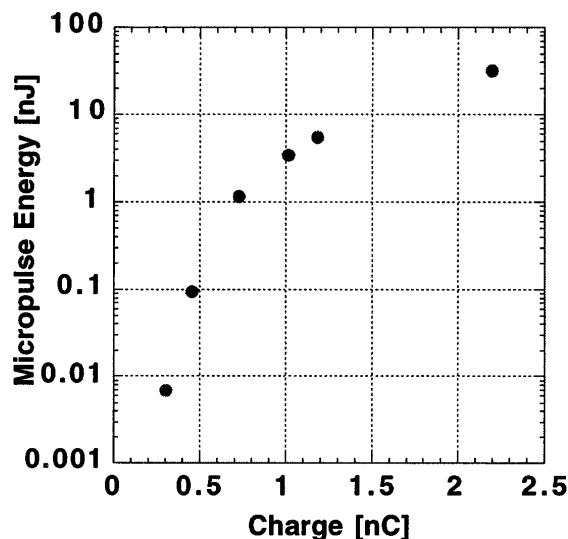


FIG. 3. Measured average FEL output energy (nJ) per micropulse for different electron beam micropulse charges (nC). The data are for single rf macropulses, representing an average of 780 individual micropulses. The error in the energy measurement is smaller than the data points—about 7%.

verified that it is always larger than 2.5×10^{-3} . Hence a smaller value of the energy spread at lower charge should not substantially modify the results shown in Fig. 4 [8,9]. GINGER simulates SASE, starting the FEL equations from a noise in the initial longitudinal distribution. To avoid doing several hundred runs to get average values for the intensity, and since the gain length is independent of the initial noise, the GINGER simulations in Fig. 4 have been normalized to the 167A data point so that the predicted growth rate can be compared with that observed.

From the GINGER results, we can evaluate the gain length at any given charge. At 2.2 nC, GINGER gives a value for the field gain length of 25 cm, much larger than the 1D gain length, as we expect given the importance of diffraction. As an additional check, we may evaluate the gain by comparing the measured value for the output intensity at 2.2 nC with the calculated spontaneous radiation intensity [15] in one gain length. Evaluating the spontaneous radiation for 2.2 nC within a solid angle Ω_c and a linewidth $1/N_u$ we obtain 1.6 pJ for the entire undulator and $i_0 = 1.6 \text{ pJ} \times (L_g/L_u)$ for the first gain length. Since in our case diffraction is strong, it is a good approximation to assume only one transverse mode is amplified. Evaluating the coupling coefficient C [10] we obtain $C \approx 0.3$. Using the measured intensity $i = (i_0/9)C \exp(2L_u/L_g) = 32 \text{ nJ}$ at 2.2 nC and solving for the gain length, we obtain a field gain length of 26 cm, consistent with GINGER. For a field gain length of 25 cm and an undulator length of 2 m we obtain a power gain of 3×10^5 .

As discussed earlier, the output intensity of an individual micropulse is a random quantity proportional to the spontaneous radiation intensity, which is itself proportional to the initial longitudinal electron bunching at the output radiation wavelength. By using a high speed (1 ns response time) liquid helium cooled Cu:Ge detector, the intensity fluctuations of individual micropulses were

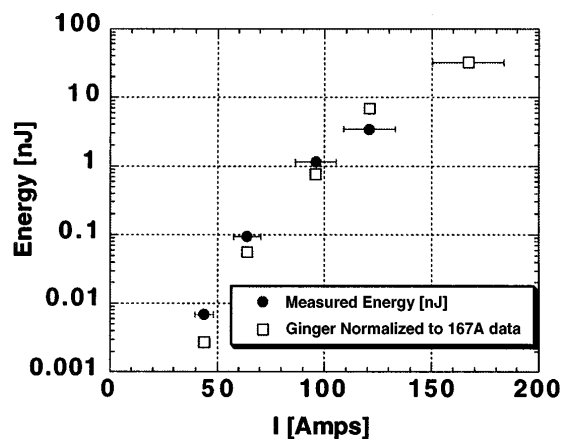


FIG. 4. Measured average FEL output energy (nJ) compared to GINGER simulations for different electron beam peak currents. The variation in beam density shown in Fig. 1 was also taken into account in the simulations. The results of the GINGER simulations have been normalized to the 167A data to allow comparison of the predicted growth rate.

measured and compared to the theoretical predictions for SASE. At 2 nC, near where we see the largest gain, the intensity distribution is shown in Fig. 5. The mean detector voltage is 76 mV with a standard deviation of 28 mV, corresponding to fluctuations on the order of 37%. Based on the work of [11,13,16–18] we expect the SASE to be completely chaotic polarized radiation, with intensity fluctuations following a gamma distribution function, and given by $1/\sqrt{M}$, where $M = (L_b/L_c)(\Omega/\Omega_c)$ and L_c is the cooperation length. At 2 nC $L_b/L_c \sim 8.8$ and a fixed aperture at the exit of the undulator limits $\Omega/\Omega_c \sim 1$; thus we expect an M value of 8.8 corresponding to fluctuations on the order of 34%. A histogram of the measured intensity fluctuations at 2 nC is given in Fig. 5 and plotted with a gamma distribution function corresponding to an M value of 8.8. For comparison, if we assume a worst case scenario, that all parameters are fluctuating within the accuracy of their respective measurements [charge (1.5%), pulse length (12%), and spot size (11%)], the fluctuations we would expect at 2 nC are on the order of 19%. The variables capable of producing a different spot size, pulse length, or energy spread for a given charge (i.e., laser alignment to the cathode, laser-rf phase, temperature of the accelerator cavity) all change on time scales several orders of magnitude longer than the micropulse separation (9.23 ns). Thus, a more reasonable estimate takes the charge dependence of pulse length and radius shown in Fig. 1 and calculates the expected fluctuations based on the change in charge from micropulse to micropulse, giving fluctuations of only 2%. The much larger fluctuations we observed (37%) are due to SASE.

We have measured the largest gain to date at an optical wavelength (12 μm) in a single pass free electron laser starting from noise. Analysis of the results shows

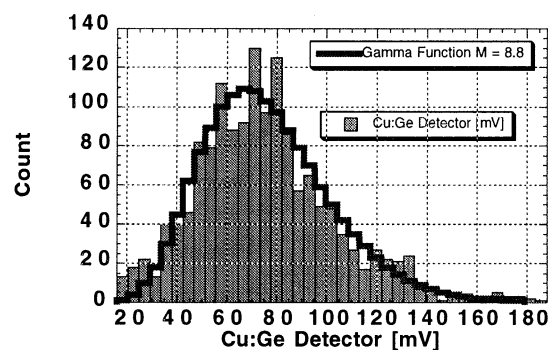


FIG. 5. Measured output intensity fluctuations for individual 2 nC micropulses compared to the predicted gamma distribution function. The mean value is 76 mV with a standard deviation of 28 mV corresponding to fluctuations on the order of 37%. Based on the FEL theory, we expect a gamma distribution function of M value 8.8 and fluctuations on the order 34%. For comparison, the fluctuations we might expect from micropulse to micropulse variations in charge are of the order of 2%. The gamma distribution function has been normalized such that the area under the curve is the same as the area of the histogram.

agreement, within the experimental errors, between the SASE-FEL theory embodied in the code GINGER and the experimental results up to gains of 3×10^5 . The magnitude and distribution of the fluctuations in output intensity agree with the predicted values for SASE radiation which is chaotic and described by a gamma distribution function.

The authors thank Kip Bishofberger, Max Cornacchia, William Fawley, Steve Lidia, Kumar Patel, John Plato, Sven Reiche, Scott Volz, and Mike Webber. Without their help and support this experiment would not have been possible. This work was supported by DOE Grant No. DE-FG03-92ER40793.

- [1] "Linac Coherent Light Source (LCLS) Design Study Report," The LCLS Design Study Group, Stanford Linear Accelerator Center (SLAC) Report No. SLAC-R-521, 1998.
- [2] J. Rossbach *et al.*, Nucl. Instrum. Methods Phys. Res., Sect. A **375**, 269 (1997).
- [3] T. Orzechowski *et al.*, Phys. Rev. Lett. **54**, 889 (1985).
- [4] M. Hogan *et al.*, Phys. Rev. Lett. **80**, 289 (1998); M. Hogan *et al.*, in *Proceedings of the Towards X-ray FEL Workshop, Garda Lake, Italy, 1997*, edited by Rodolfo Bonifacio and William A. Barletta, AIP Conf. Proc. No. 413 (AIP, New York, 1997).
- [5] R. Prazeres *et al.*, Phys. Rev. Lett. **78**, 2124 (1997).
- [6] M. Babzien *et al.*, Phys. Rev. E **57**, 6093 (1998); I. Ben Zvi (private communication).
- [7] D. C. Nguyen *et al.*, Phys. Rev. Lett. **81**, 810 (1998).
- [8] R. Bonifacio, C. Pellegrini, and L. Narducci, Opt. Commun. **50**, 373 (1984).
- [9] K.-J. Kim, Nucl. Instrum. Methods Phys. Res., Sect. A **250**, 396 (1986); J.-M. Wang and L.-H. Yu, Nucl. Instrum. Methods Phys. Res., Sect. A **250**, 484 (1986); S. Krinsky and L. H. Yu, Phys. Rev. A **35**, 3406 (1987).
- [10] G. T. Moore, Nucl. Instrum. Methods Phys. Res., Sect. A **239**, 19 (1985); E. T. Scharlemann, A. M. Sessler, and J. S. Wurtele, Phys. Rev. Lett. **54**, 1925 (1985); M. Xie and D. A. G. Deacon, Nucl. Instrum. Methods Phys. Res., Sect. A **250**, 426 (1986); K.-J. Kim, Phys. Rev. Lett. **57**, 1871 (1986); L.-H. Yu, S. Krinsky, and R. Gluckstern, Phys. Rev. Lett. **64**, 3011 (1990).
- [11] M. C. Teich *et al.*, Phys. Rev. Lett. **65**, 3393 (1990).
- [12] James Rosenzweig (private communication).
- [13] R. Bonifacio *et al.*, Phys. Rev. Lett. **73**, 70 (1994).
- [14] William Fawley (private communication).
- [15] *Laser Handbook*, edited by W. Colson, C. Pellegrini, and A. Renieri (North-Holland, Amsterdam, 1990).
- [16] E. L. Saldin, E. A. Schneidmiller, and M. V. Yurkov, "Statistical Properties of Radiation from VUV and X-ray Free Electron Laser," DESY Report No. TESLA-fel 97-02, 1997.
- [17] K. J. Kim, "Temporal and Transverse Coherence of Self-Amplified Spontaneous Emission," LBNL Report No. LBNL-40672, 1997.
- [18] *Statistical Optics*, edited by J. W. Goodman (Wiley, New York, 1985).